AMERICAN SOCIETY FOR MICROBIOLOGY | Journal of Virology®

VIRUS-CELL INTERACTIONS

Mice Expressing Minimally Humanized CD81 and Occludin Genes Support Hepatitis C Virus Uptake *In Vivo*

Qiang Ding,[a] Markus von Schaewen,[a] Gabriela Hrebikova,[a] Brigitte Heller,[a] Lisa Sandmann,[b] Mario Plaas,[c] Alexander Ploss[a]

Princeton University, Department of Molecular Biology, Lewis Thomas Laboratory, Princeton New Jersey, USA[a]; Hannover Medical School, Hannover, Germany[b]; University of Tartu, Faculty of Medicine, Institute of Biomedicine and Translational Medicine, Laboratory Animal Centre, Tartu, Estonia[c]

ABSTRACT Hepatitis C virus (HCV) causes chronic infections in at least 150 million individuals worldwide. HCV has a narrow host range and robustly infects only humans and chimpanzees. The underlying mechanisms for this narrow host range are incompletely understood. At the level of entry, differences in the amino acid sequences between the human and mouse orthologues of two essential host factors, the tetraspanin CD81 and the tight junction protein occludin (OCLN), explain, at least in part, HCV's limited ability to enter mouse hepatocytes. We have previously shown that adenoviral or transgenic overexpression of human CD81 and OCLN facilitates HCV uptake into mouse hepatocytes *in vitro* and *in vivo*. In efforts to refine these models, we constructed knock-in mice in which the second extracellular loops of CD81 and OCLN were replaced with the respective human sequences, which contain the determinants that are critical for HCV uptake. We demonstrate that the humanized CD81 and OCLN were expressed at physiological levels in a tissue-appropriate fashion. Mice bearing the humanized alleles formed normal tight junctions and did not exhibit any immunologic abnormalities, indicating that interactions with their physiological ligands were intact. HCV entry factor knock-in mice take up HCV with an efficiency similar to that in mice expressing HCV entry factors transgenically or adenovirally, demonstrating the utility of this model for studying HCV infection *in vivo*.

IMPORTANCE At least 150 million individuals are chronically infected with hepatitis C virus (HCV). Chronic hepatitis C can result in progressive liver disease and liver cancer. New antiviral treatments can cure HCV in the majority of patients, but a vaccine remains elusive. To gain a better understanding of the processes culminating in liver failure and cancer and to prioritize vaccine candidates more efficiently, small-animal models are needed. Here, we describe the characterization of a new mouse model in which the parts of two host factors that are essential for HCV uptake, CD81 and occludin (OCLN), which differ between mice and humans, were humanized. We demonstrate that such minimally humanized mice develop normally, express the modified genes at physiological levels, and support HCV uptake. This model is of considerable utility for studying viral entry in the three-dimensional context of the liver and to test approaches aimed at preventing HCV entry.

KEYWORDS animal models, hepatitis C virus, viral entry, viral hepatitis

Received 6 September 2016 **Accepted** 23 November 2016

Accepted manuscript posted online 7 December 2016

Citation Ding Q, von Schaewen M, Hrebikova G, Heller B, Sandmann L, Plaas M, Ploss A. 2017. Mice expressing minimally humanized CD81 and occludin genes support hepatitis C virus uptake *in vivo*. J Virol 91:e01799-16. https://doi.org/10.1128/JVI.01799-16.

Editor Michael S. Diamond, Washington University School of Medicine

Address correspondence to Alexander Ploss, aploss@princeton.edu.

Hepatitis C virus (HCV) is a positive-sense, single-stranded RNA virus belonging to the *Flaviviridae* family, genus *Hepacivirus* (1). HCV progresses to persistent infection in 70 to 80% of those individuals who become acutely infected (2). Chronic carriers are at risk of developing fibrosis, cirrhosis, and hepatocellular carcinoma (HCC) if they remain untreated. Over a few years, very potent directly acting antivirals (DAAs) which can cure

HCV infection in the majority of patients were approved (reviewed in reference 3). Despite these tremendous successes, the HCV disease burden has only marginally decreased, in part due to the limited availability of curative drug regimens and the lack of a protective vaccine. It also remains incompletely understood why individuals who have been successfully treated and have progressed to advanced fibrosis remain at an elevated risk for developing HCCs. Both vaccine development and improving our understanding of HCV pathogenesis would greatly benefit from a small-animal model of hepatitis C (4).

HCV's host range is limited to productive infection in humans and chimpanzees. It remains mechanistically incompletely understood why HCV has such a narrow host range. In mouse cells, the HCV life cycle is blocked or inefficiently supported at multiple steps, in particular, viral entry and HCV RNA replication (reviewed in reference 5). A surprisingly large number of host factors have been shown to be important in the uptake of HCV into human hepatocytes, including glycosaminoglycans (GAGs) present on heparan sulfate proteoglycans (HSPGs) (6), low-density-lipoprotein receptor (LDLR) (7), CD81 (8), scavenger receptor class B member 1 (SCARB1) (9), the tight junction (TJ) proteins claudin-1 (CLDN1) (10) and occludin (OCLN) (11, 12), the receptor tyrosine kinases epidermal growth factor receptor (EGFR) and ephrin receptor A2 (EphA2) (13), the cholesterol transporter Niemann-Pick C1-like 1 (NPC1L1) (14), transferring receptor 1 (TfR1) (15), the cell death-inducing DFFA-like effector b (CIDEB) (16), and E-cadherin (17). Of those, differences in the sequences of CD81 and OCLN between the murine and human orthologues can at least in part explain the lower efficiency of HCV uptake by rodent versus human cells. Specifically, residues contained in the second extracellular loops of CD81 and OCLN, which have previously been shown to be critical for HCV entry, are not conserved (18, 19). We have previously demonstrated that ectopic overexpression of human CD81 and OCLN enables uptake by mouse cell lines of both hepatic and nonhepatic origin (12, 20). Both CLDN1 and SCARB1 are also required, but orthologues from other nonhuman species, such as mouse or hamster, have been shown to support HCV entry. When CD81 and OCLN are overexpressed through adenoviral delivery (21) or transgenically (22), HCV can enter mouse hepatocytes *in vivo*. While such genetically humanized mice have proven to be useful to study HCV entry and to test approaches focusing on blocking HCV entry (21, 23–25), a shortcoming is the unphysiologically high expression level achieved by these heterologous expression approaches. Also, neither CD81 nor OCLN is uniquely expressed in the liver; rather, CD81 and OCLN are expressed on all nucleated cells and all tight junctions, respectively. Thus, it would be desirable to refine these models and monitor HCV uptake under conditions when both entry factors are expressed at physiological levels. To address this point, we constructed a novel genetically humanized mouse model in which the second extracellular loops of CD81 and OCLN were humanized. Mice harboring the humanized alleles developed normally and did not exhibit any overt phenotype. Transcripts of these chimeric alleles were expressed at physiological levels in a pattern that resembled expression of the wild-type alleles. The humanized CD81 (mCD81/hEL2[h/h]) molecule appears to facilitate the endogenous functions of murine CD81 (mCD81), as the chimeric mice did not show any of the defects in B cell development observed in CD81-deficient mice. In mice containing the humanized OCLN (mOCLN/hEL2[h/h]) allele, tight junctions formed normally, indicating that the mutant version can carry out the physiological functions of OCLN as part of TJ complexes. We further demonstrate that mice expressing both the humanized CD81 and OCLN alleles support the uptake of HCV in a dose-dependent manner. HCV uptake was similar to that in mice administered adenoviruses expressing CD81 and OCLN and HCV entry factor transgenic mice. This new HCV entry factor knock-in model will be useful for future mechanistic studies focusing on HCV entry.

RESULTS

Physiological expression of humanized CD81 and OCLN transcripts across multiple tissues. HCV entry factors are expressed at finely controlled levels in the liver

and other tissues. In order to achieve more physiological expression, we undertook a knock-in approach. The low efficiency of entry mediated by mCD81 and murine OCLN (mOCLN) has been mapped to divergence in the respective second extracellular loops (18, 19). Thus, we reasoned that minimal replacements might be sufficient to permit HCV infection while preserving mouse-specific intracellular domains. The large extracellular loop (amino acids 115 to 202) of mCD81 was replaced by knocking in human exons 6 and 7 (Fig. 1A and C). Similarly, exon 3 of mOCLN, which encodes the second extracellular loop, was replaced with the human sequence (Fig. 1B and D). Chimeric founder mice, termed mCD81/hEL2[h/m] and mOCLN/hEL2[h/m], were identified and backcrossed to mice of the C57BL/6 background. The offspring did not show any gross phenotype and were born in the expected Mendelian ratios. CD81 is expressed in all nucleated cells, and OCLN is an integral molecule of all tight junction complexes. To ascertain a similarly broad tissue expression of the humanized allele, we subjected brain, skin, intestine, stomach, heart, lung, spleen, kidney, and liver tissue of wild-type, mCD81/hEL2[h/h], and mOCLN/hEL2[h/h] mice to quantitative reverse transcription-PCR (RT-qPCR) analysis using allele specific-primers (Table 1). Both mutant mouse strains showed levels of CD81 or OCLN tissue expression largely similar to those in wild-type mice (Fig. 2A and B), with slightly lower transcript levels being seen in liver, spleen, and lung tissue. We did not observe any difference in the level of expression in mice homozygous or heterozygous (data not shown) for the respective chimeric alleles.

mCD81/hEL2[h/h] and mOCLN/hEL2[h/h] mice do not show any overt pathophysiological phenotype. Besides its role as an entry factor for human hepatotropic pathogens, such as HCV and *Plasmodium falciparum* (26), CD81 is a cell surface molecule expressed on many cell types and associated with the CD19/CD21/Leu13 signal-transducing complex on B cells. Conceivably, humanizing the second extracellular loop of mouse CD81 may interfere with its endogenous functions, and mice with humanized CD81 could possibly resemble phenotypically CD81-deficient ($CD81^{-/-}$) mice. $CD81^{-/-}$ mice are reported to have decreased expression of CD19 and reduced numbers of peritoneal B1 cells (27–29). Thus, we compared lymphocyte frequencies in wild-type and mCD81/hEL2[h/h] mice. CD8 and CD4 T cell frequencies were unaltered in the thymus (Fig. 3A, top) and the spleen (Fig. 3A, top) of both mutant and wild-type animals. mCD81/hEL2[h/h] mice had normal frequencies of IgM-negative (IgM^-) $B220^{lo}$ cells (pro-B cells), IgM^- $B220^{int}$ cells (pre-B cells), IgM-positive (IgM^+) $B220^{int}$ cells (immature B cells), and IgM^+ $B220^{hi}$ cells (mature B cells), and CD19 expression was normal (Fig. 3B). Thus, all stages of B cell development in the bone marrow appeared to be normal. Furthermore, besides a slight (2-fold) increase in the frequency of B1a cells in the peritoneum, the overall numbers of B1 and B2 cells were similar in wild-type and mCD81/hEL2[h/h] mice (Fig. 3C).

OCLN is an integral membrane protein with four transmembrane domains that is exclusively localized at TJ strands. The two extracellular loops form homotypic interactions to stabilize TJs (30). To ensure that humanization of the second extracellular loop does not affect OCLN physiological functions, we subjected liver tissue from mOCLN/hEL2[h/h] and wild-type mice to histological analysis. It was previously shown that OCLN-deficient ($OCLN^{-/-}$) mice exhibit histological abnormalities in several tissues, i.e., chronic inflammation and hyperplasia of the gastric epithelium, calcification in the brain, testicular atrophy, loss of cytoplasmic granules in striated duct cells of the salivary gland, and thinning of the compact bone (31). In contrast, mOCLN/hEL2[h/h] mice developed normally, nursed their offspring, and did not show any of the histopathological features of OCLN-deficient mice. Staining of OCLN, claudin-1 (CLDN1), and zona occludens 1 (ZO-1), all of which are TJ components, in liver sections was indistinguishable between mOCLN/hEL2[m/m] and mOCLN/hEL2[h/h] mice (Fig. 3D). Overall, these data demonstrate that humanization of the second extracellular loop of both CD81 and OCLN does not seem to impair the endogenous functions.

Dose-dependent uptake of HCV into mCD81/hEL2[h/h] mOCLN/hEL2[h/h] mice. Next we aimed to test whether the minimal humanization of the murine CD81 and

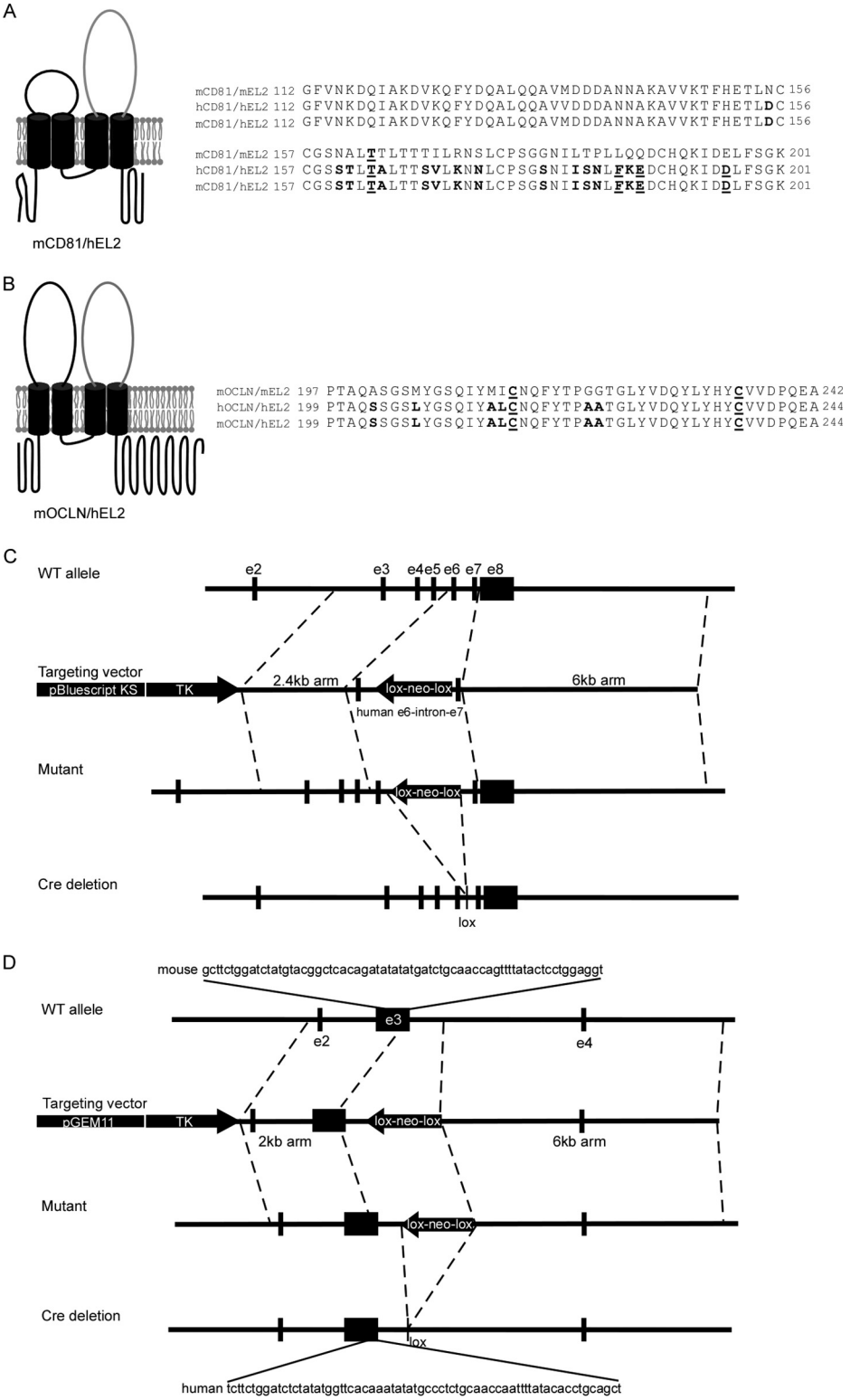

FIG 1 Schematic representation of humanized CD81 and OCLN alleles and native tissue expression profiles of humanized CD81 and OCLN alleles. (A and B) Schematic representation of the mCD81/hEL2 (A) and mOCLN/hEL2 (B) proteins and alignments of sequences of the second extracellular loops of mouse, human, and humanized proteins. Differences between the human and mouse sequences are in bold, and the residues that were shown to be critical for HCV uptake are underlined. (C and D) Schematics detailing the targeting strategy used to generate the mCD81/hEL2[h/h] (C) or mOCLN/hEL2[h/h] knock-in mice (D). WT, wild type.

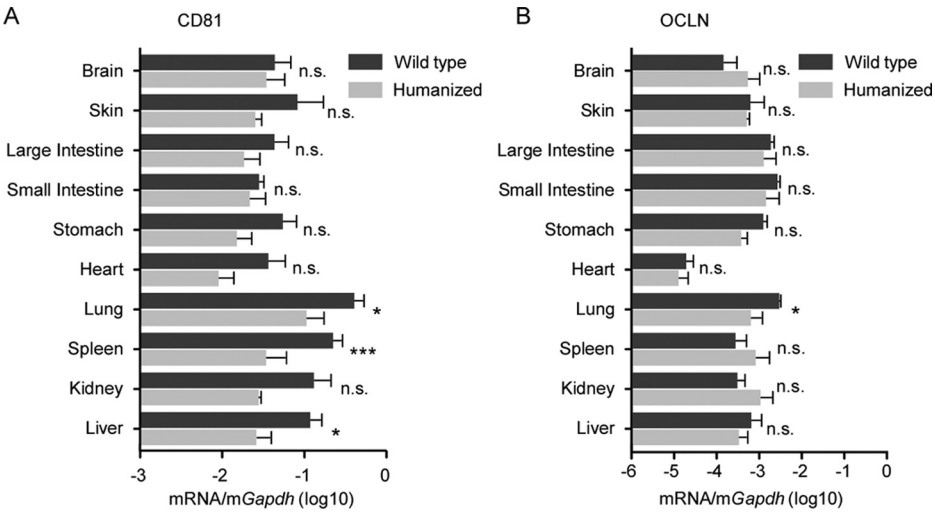

FIG 2 Expression of humanized CD81 and OCLN alleles in entry factor knock-in mice. The quantities of the wild-type and humanized transcripts in different tissues of mCD81/hEL2[h/h] (A) and mOCLN/hEL2[h/h] mice (B) are shown. Data are shown as means ± SDs from at least 3 experiments. Statistical analysis was performed using a one-tailed Student *t* test. *, $P < 0.05$; ***, $P < 0.001$), n.s., not statistically significant.

OCLN alleles would be sufficient to facilitate viral uptake into murine hepatocytes *in vivo*. We have previously shown that adenoviral delivery or transgenic expression of full-length human CD81 and OCLN is sufficient to enable HCV glycoprotein-mediated uptake (21, 22, 32). To assess the ability of mCD81/hEL2[h/h] mOCLN/hEL2[h/h] double-knock-in mice to support HCV uptake *in vivo*, we employed a cellularly encoded reporter which can be activated by coexpression of Cre recombinase (21, 32, 33). mCD81/hEL2[h/h] mOCLN/hEL2[h/h] mice were intercrossed with the Gt(ROSA)26Sor$^{tm1(Luc)Kaelin}$ (Rosa26-Fluc) mouse strain (34) harboring a loxP-flanked luciferase (luc) reporter. The resultant offspring were infected with increasing tissue culture infectious doses (TCID) of a bicistronic HCV genome expressing Cre recombinase (BiCre-Jc1; abbreviated HCV-Cre), which is designed to activate a luminescent reporter. *In vivo* luminescence imaging demonstrated a significant increase in relative photon flux in the entry factor double-knock-in (EFKI) mice at 72 h postinfection (Fig. 4A and B). The signal increased roughly 3-fold over the background following infection with the highest dose tested (3×10^7 $TCID_{50}$) (Fig. 4B), demonstrating that uptake efficiency is dose dependent. This dose dependency is consistent with what has previously been reported in HCV entry factor transgenic mice (22) or animals expressing human CD81 and OCLN (21) in their livers after adenoviral delivery. Of note, reporter activity was largely limited to the liver, and we observed only a slight activation of the reporter in the spleen and kidney and not in other, nonhepatic tissues, where the humanized alleles may also be expressed (Fig. 4C).

mCD81/hEL2[h/h] mOCLN/hEL2[h/h] double-knock-in mice support HCV entry at levels similar to those in mice expressing adenovirally or transgenically delivered human CD81 and OCLN. Lastly, we aimed to compare whether the efficiency of HCV entry into murine hepatocytes differed across animals in which human(ized) CD81 and OCLN is (over)expressed by different means. mCD81/hEL2[h/h] mOCLN/hEL2[h/h] mice and animals expressing full-length human CD81 and OCLN adenovirally off a cytomegalovirus (CMV) promoter or transgenically off a mouse albumin promoter (all on the Rosa26-Fluc background) were injected with 2×10^7 $TCID_{50}$ of BiCre-Jc1, and the bioluminescence signal was quantified after 72 h (Fig. 5). The bioluminescence signal increased 2- to 3-fold over the background and was largely equivalent across all three entry models. Collectively, these data demonstrate that minimal humanization of the second extracellular loops is sufficient to facilitate the entry of HCV into hepatocytes but presumably not into extrahepatic tissues.

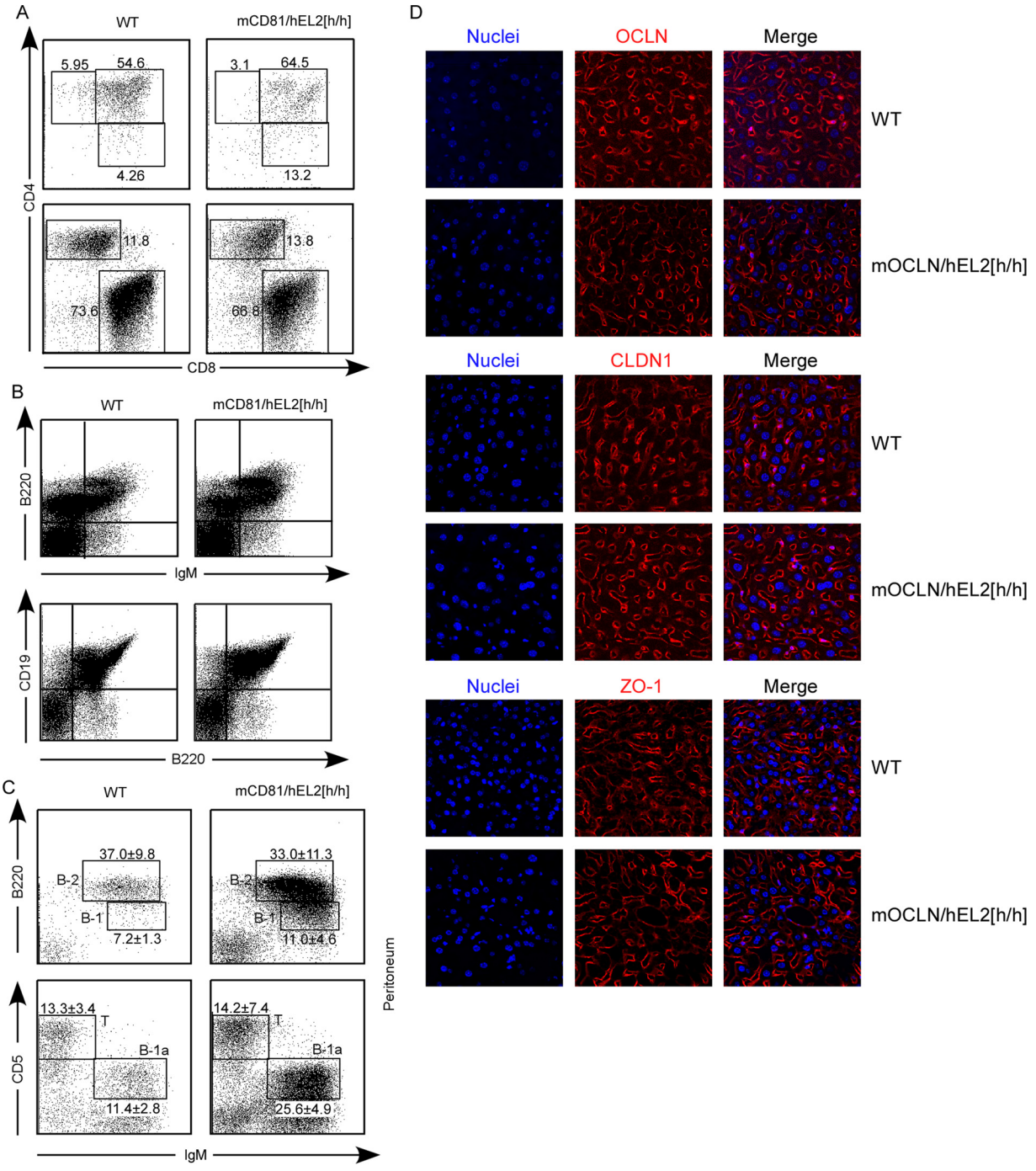

FIG 3 Humanization of the second extracellular loops of mCD81 and mOCLN does not interfere with the endogenous functions of these molecules. (A) Flow cytometry analysis of thymocytes (top) and splenocytes (bottom) from wild-type (WT) and mCD81/hEL2[h/h] mice. (B and C) Flow cytometry analysis of bone marrow cells (B) and peritoneal lavage cells (C) from wild-type and mCD81/hEL2[h/h] mice. Representative flow cytometric plots and frequencies (mean ± SD) are shown. (D) Confocal microscopy images of thin sections (6 μm) of livers from mOCLN/hEL2[m/m] (wild-type) or mOCLN/hEL2[h/h] mice stained with antibodies against mouse OCLN (top two rows), CLDN1 (middle two rows), or ZO-1 (bottom two rows). To visualize nuclei (blue), sections were stained with Hoechst dye.

DISCUSSION

The use of great apes in biomedical research is heavily scrutinized, and either work with these animals has been banned or federal funding for such work has ceased. In the search for alternative models, a variety of approaches have been taken (reviewed in reference 4). Some studies suggested that tree shrews (*Tupaia belangeri*) can become chronically infected with HCV (35) (36, 37) and even develop fibrosis (37), but this

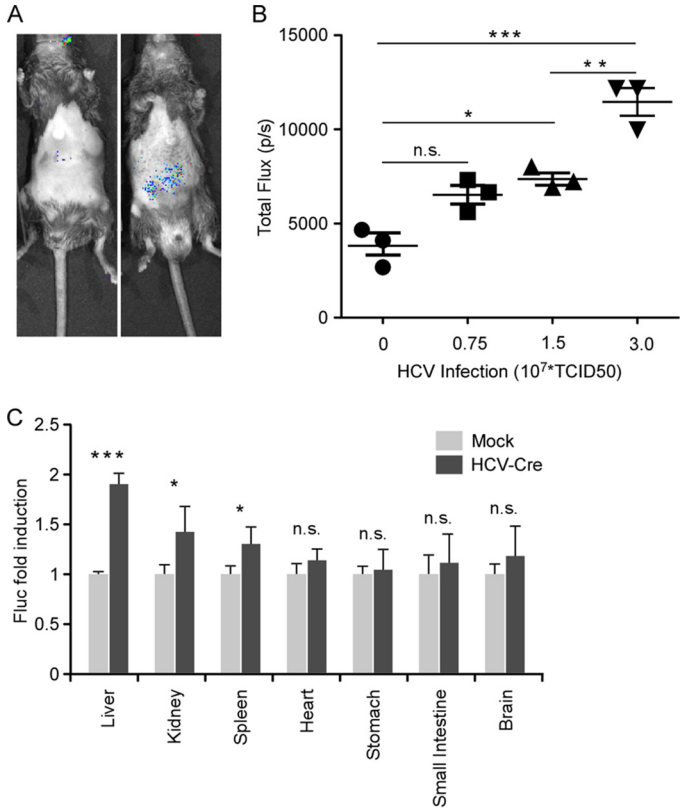

FIG 4 Activation of the bioluminescent reporter in HCV entry factor knock-in mice is dependent on HCV dose. (A) Representative images of mock-infected mice (left) or HCV-Cre-infected mCD81/hEL2[h/h] mOCLN/hEL2[h/h] Rosa26-Fluc mice (right). (B) mCD81/hEL2[h/h] mOCLN/hEL2[h/h] Rosa26-Fluc mice ($n = 3$) were injected with various doses of HCV-Cre, as indicated. Data represent means ± SDs. Statistical significance was calculated by one-way analysis of variance with Bonferroni's multiple-comparison test. p/s, number of photons per second. (C) Luminescent reporter activation across different tissues. The indicated tissues from mCD81/hEL2[h/h] mOCLN/hEL2[h/h] Rosa26-Fluc mice (mock infected or HCV-Cre infected) were extracted, and luminescent activity was measured *ex vivo*. All bioluminescent signals were quantified at 72 h following infection. Data represent means ± SDs. Statistical analysis was performed using a one-tailed Student *t* test. *, $P < 0.05$; **, $P < 0.01$; ***, $P < 0.001$; n.s., not statistically significant.

model has not found widespread use yet. HCV-like viruses have been more recently identified in a variety of species, including horses, dogs, rats, and mice, but it is unclear whether such related hepaciviruses cause clinical symptoms similar to those caused by HCV and, thus, whether these animals could be used as surrogate models (38). A variety of other approaches focusing on modifying the (murine) host environment in a way that it becomes more conducive to HCV infection have been pursued. Mice engrafted with human hepatocytes have been shown to be susceptible to HCV (25, 39–41). Despite their utility for studying a variety of human hepatotropic pathogens, such human liver chimeric mice have not found widespread use, as they can be produced only at a low throughput, and their generation is expensive and requires considerable technical skills. Alternatively, systematic analysis and identification of some of the barriers to the interspecies transmission of HCV to classically nonpermissive species, in particular, mice, have spurred genetic humanization efforts. After the discovery that human CD81 and OCLN comprise the minimal set of human-specific factors required for viral entry into mouse cell lines (12), it was demonstrated that adenovirally mediated (21) or transgenic (22) overexpression of these factors enabled HCV entry *in vivo*. The caveats to the use of these two systems are the nonphysiologically high level and exclusive expression in hepatocytes. The levels of adenovirally mediated expression of human CD81 and OCLN can exceed the endogenous levels of expression in the mouse 100- to 1,000-fold (21), and transgenic expression under the control of a mouse albumin

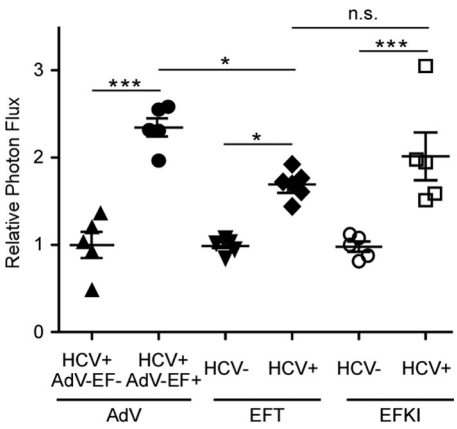

FIG 5 Similar uptake efficiency of HCV into different mouse models expressing HCV entry factors. Rosa26-Fluc mice were injected with 1×10^{11} adenovirus (AdV) CD81 and OCLN particles, and 24 h later these mice, Alb-hCD81/hOCLN entry factor transgenic (EFT) Rosa26-Fluc mice, and mCD81/hEL2[h/h] mOCLN/hEL2[h/h] entry factor knock-in (EFKI) Rosa26-Fluc mice were infected with 2×10^7 $TCID_{50}$ of HCV ($n = 5$). The bioluminescent signal was quantified at 72 h following infection. Data represent means ± SDs. Statistical significance was calculated by one-way analysis of variance with Bonferroni's multiple-comparison test. *, $P < 0.05$; ***, $P < 0.001$; n.s., not statistically significant.

promoter still results in 10-fold overexpression (10). Furthermore, the intracellular domains of the full-length human orthologues may interact less efficiently with the murine proteins that usually bind to their respective adaptor proteins. To address these shortcomings, the second extracellular loops of mouse CD81 and OCLN were humanized. mCD81/hEL2[h/h] mOCLN/hEL2[h/h] double-knock-in mice develop normally, and the minimal humanization of the loop appears to be sufficient to facilitate HCV uptake into murine hepatocytes. Humanization of the second extracellular loops does not impair the respective endogenous functions of CD81 and OCLN *in vivo*. Conceivably, the phenotype of these mutant mice would have resembled that of animals with targeted disruptions of CD81 (27–29) and OCLN (31), which were previously reported. However, our analysis demonstrates that the loop replacements do not noticeably alter B lymphocyte or tight junction biology.

On the basis of several clinical conditions, it has previously been speculated that extrahepatic sites of HCV infection may exist. For example, a potential involvement of the central nervous system (CNS) was based on observations that chronic HCV carriers frequently become encephalopathic and develop neuropsychiatric disorders (42). HCV RNA has been detected in brain tissue from HCV-infected individuals (43), but contamination of samples collected postmortem after the blood-brain barrier has broken down is a confounding problem. Additionally, evidence that the CNS is a putative HCV reservoir stemmed from *in vitro* studies showing that HCV can enter human peripheral neuroblastoma and neuroepithelioma cells *in vitro* (44, 45). However, currently there is no direct evidence of active HCV RNA replication in cells derived from the CNS of HCV-infected patients. HCV RNA has also been shown to be associated with various hematopoietically derived cells, such as B and T lymphocytes, monocytes, and dendritic cells. This led to the hypothesis that HCV may infect these populations, triggering the lymphoproliferative disorders which are frequently observed in chronic HCV carriers. However, attempts to infect human peripheral blood mononuclear cells (PBMCs) largely with cell culture-derived HCV failed (46), suggesting that HCV particles and/or RNA may adhere to these cells but not efficiently enter them. HCV proteins have also been detected in epithelial cells from intestinal tissue specimens collected from HCV-infected patients (47), and *in vitro* experiments provided evidence that they can enter cells of the Caco-2 epithelium-derived colorectal adenocarcinoma cell line (48).

It remains controversial whether HCV infects nonparenchymal cells *in vivo* or whether infection of such putative extrahepatic sites has any clinical relevance. CD81 is ubiquitously expressed in almost all nucleated cells, and OCLN is part of all tight

TABLE 1 Primers used for RT-qPCR analysis

Gene	Sequence	
	Forward primer	Reverse primer
mCD81/hEL2	CCAAGGCTGTGGTGAAGACTTTC	TGTTCTTGAGCACTGAGGTGGTC
mCD81/mEL2	CCAAGGCTGTGGTGAAGACTTTC	GGCTGTTCCTCAGTATGGTGGTAG
mOCLN/hEL2	AAATTGGTTGCAGAGGGCATAT	GTGTTTATTGCCACGATCGTGT
mOCLN/mEL2	AAACTGGTTGCAGATCATATAT	GTGTTTATTGCCACGATCGTGT
gapdh[a]	ACGGCCAAATCCGTTCACACC	ACGGCCGCATCTTCTTGTGCA

[a]*gapdh*, the gene for glyceraldehyde-3-phosphate dehydrogenase.

junction complexes present in polarized cell layers. Interestingly, alternative splice forms of OCLN which are differentially expressed across tissues have been described, and thus, these might contribute to HCV tissue tropism (49). However, while CLDN1 and SCARB1 are expressed in a variety of nonhepatic tissues, the combination of both at high levels occurs only in the liver, which may largely contribute to HCV's tissue specificity at the entry level. Consistently, we observed HCV uptake primarily in the liver and to a much lesser extent in the spleen and kidneys of HCV-infected double-knock-in mice. The limited evidence for HCV uptake in nonhepatic tissues may, however, be because of the limits of detection of the assays employed here. In future studies, our model may lend itself to further exploration of HCV tissue tropism.

MATERIALS AND METHODS

Generation of mice expressing humanized CD81 and OCLN alleles. Gene-targeting constructs coding mCD81/hEL2 (mouse exons 6 and 7 of the CD81 gene coding the extracellular loop named EL2 were replaced with human exons 6 and 7, respectively) and mOCLN/hEL2 (a part of exon 3 of the mouse OCLN gene that encodes extracellular loop 2 was replaced with a part of human exon 3, what encodes EL2) were transformed into ES cells (129S6SvEv mouse genetic background) by standard electroporation (Fig. 1C and D). Correct targeting of the alleles in ES cell clones was analyzed by PCR and verified by DNA sequencing. After the number of chromosomes was checked, *in vitro* Cre recombination was performed to cut off the Neo-tk selection cassette between loxP sites. Correctly targeted ES cell clones containing the mCD81/hEL2 or mOCLN/hEL2 alleles were microinjected into C57BL6/J mouse blastocysts. Chimeric mice were initially crossed with C57BL6/J mice (in the case of mOCLN/hEL2) or with 129S6SvEv mice (in the case of mCD81/hEL2) to obtain germ line offspring. mOCLN/hEL2 and mCD81/hEL2 knock-in mice were subsequently crossed for 10 generations to mice of the C57BL/6 background. Experiments were performed in accordance with a protocol reviewed and approved by the Institutional Animal Care and Use Committee of the University of Tartu.

Animals and cell lines. The generation of mice expressing human HCV entry factors under the control of a liver-specific albumin promoter was previously described (22). Gt(ROSA)26Sor$^{tm1(Luc)Kaelin}$ (Rosa26-Fluc) (34) were obtained from The Jackson Laboratory and backcrossed for 10 generations to mice of the C57BL/6 background. Rosa26-Fluc mice contain the firefly luciferase (Fluc) gene inserted into the Gt(ROSA)26Sor locus. Expression of the luciferase gene is blocked by a loxP-flanked STOP fragment placed between the Fluc sequence and the Gt(ROSA)26Sor promoter. Cre recombinase-mediated excision of the transcriptional stop cassette results in luciferase expression in Cre-expressing tissues. Mice were bred and maintained at the Laboratory Animal Resource Center of Princeton University according to guidelines established by the Institutional Animal Committee. Huh-7.5 cells (kindly provided by Charles Rice, The Rockefeller University) and Huh-7.5.1 cells (kindly provided by Frank Chisari, The Scripps Research Institute) were maintained in Dulbecco modified Eagle medium (DMEM) supplemented with 5% fetal bovine serum (FBS) and 1% nonessential amino acids (NEAA), and 293T cells (American Type Culture Collection [ATCC]) and HEK293 cells (ATCC) were maintained in DMEM supplemented with 10% FBS and 1% NEAA.

Quantification of the humanized CD81 and OCLN transcripts by RT-qPCR. Total RNA was isolated from mouse brain, heart, large and small intestine, kidney, liver, lung, skin, spleen, and stomach using an RNeasy minikit (Qiagen, Valencia, CA). cDNA was synthesized from 0.5 μg RNA using a SuperScript III first-strand synthesis system (Invitrogen, Carlsbad, CA) according to the manufacturer's instructions. Quantitative PCR was performed with a Step One Plus RT-PCR system (Applied Biosciences) using an Applied Biosystems SYBR green PCR master mix (Warrington, UK) and the primer pairs listed in Table 1.

HCV generation and infections. Huh-7.5.1 or Huh-7.5 cells were electroporated with *in vitro*-transcribed full-length HCV RNA of the BiCre-Jc1 genomes (21). At 72 h postelectroporation, the medium was replaced with DMEM containing 1.5% FBS, and supernatants were harvested every 6 h starting from 72 h postelectroporation. Pooled supernatants were clarified by centrifugation at 1,500 $\times$ *g*, filtered through a 0.45-μm-pore-size bottle-top filter (Millipore), and concentrated using a stirred cell (Millipore). Viral titers ($TCID_{50}$) were determined using Huh-7.5 cells as previously described (50).

Production of recombinant adenoviruses. Adenovirus stocks encoding human HCV entry factors (CD81 and OCLN) were generated as previously described (51). Briefly, adenovirus constructs were transfected into HEK293 cells (ATCC) using the calcium phosphate method. Transfected cell cultures were

maintained until the cells exhibited a complete cytopathic effect (CPE), and then the cells were harvested and freeze-thawed to get the cell lysate. This cell lysate was then used to infect HEK293 cells. Once the infected cells exhibited CPE, either the cell pellets were harvested for adenoviral purification or the cells and media were freeze-thawed for use in future infections. For virus purification, cell pellets were resuspended in 0.01 M sodium phosphate buffer, pH 7.2, and lysed in 5% sodium deoxycholate, followed by DNase I digestion. The lysates were centrifuged, and the supernatant was layered onto a 1.2- to 1.46-g/ml CsCl gradient and then spun at 23,000 rpm on a Beckman Optima 100K-Ultra centrifuge using an SW28 spinning-bucket rotor (Beckman Coulter). Adenovirus bands were isolated and further purified on a second CsCl gradient using an SW41.Ti spinning-bucket rotor. The resulting purified adenoviral bands were isolated using an 18.5-guage needle and twice dialyzed against 4% sucrose. Adenovirus concentrations were measured at 10^{12} times the dilution factor times the reading of the optical density at 260 nm on a FLUOstar Omega plate reader (BMG Labtech). Adenovirus stocks were aliquoted and stored at −80°C.

Antibodies and flow cytometry analysis. Bone marrow, spleen, and thymus were harvested from mice of the genotypes indicated above and homogenized through a cell strainer. For the isolation of splenocytes, the spleen was digested in collagenase-containing medium for 30 min at 37°C prior to homogenization. Peritoneal cavity cells were obtained by peritoneal lavage with ice-cold phosphate-buffered saline (PBS). Cell suspensions were first incubated with an anti-CD16/CD32 monoclonal antibody (catalog number 553141; clone 2.4G2; BD Pharmingen) for 15 min at 4°C. Following the blocking step, cells were incubated with fluorochrome- or biotin-conjugated antibodies for 30 min at room temperature. Splenocytes, bone marrow, and peritoneal cavity cells were stained with fluorescein isothiocyanate (FITC)-conjugated anti-mouse CD5 (1:100; clone 53-7.3; catalog number 100605; BioLegend), peridinin chlorophyll protein-Cy5.5-conjugated anti-mouse CD19 (1:100; clone 1D3; catalog number 45-0193-82; eBioscience), allophycocyanin (APC)-conjugated anti-human CD81 (1:100; clone JS-81; catalog number 551112; BD Pharmingen), Alexa Fluor 700-conjugated anti-mouse CD45R/B220 (1:100; clone RA3-6B2; catalog number RM2629; Invitrogen), APC-Cy7-conjugated anti-mouse IgM (1:100; clone RMMM-1; catalog number 406515; BioLegend), biotin-conjugated anti-mouse CD81 (1:100; clone 2F7; catalog number NBP1-28138; Novus Biologicals), and phycoerythrin (PE)-Cy7-conjugated anti-mouse CD11b (1:199; clone M1/70; catalog number 15-0112-82; eBioscience). Splenocytes and thymocytes were stained with FITC-conjugated anti-mouse CD81 (1:50; clone EAT2; catalog number 130-094-864; Miltenyi Biotec), PE-Texas Red-conjugated anti-mouse CD4 (1:50; clone GK1.5; catalog number ab51467; Abcam), APC-conjugated anti-human CD81 (1:100; clone JS-81; catalog number 551112; BD Pharmingen), Alexa Fluor 700-conjugated anti-mouse CD45R/B220 (1:100; clone RA3-6B2; catalog number RM2629; Invitrogen), APC-Cy7-conjugated anti-mouse CD3 (1:100; clone 145-2C11; catalog number 557596; BD Pharmingen), and PE-conjugated anti-mouse CD8 (1:100; clone 53-6.7; catalog number 553089; BD Pharmingen). Biotin-conjugated reagents were counterstained with streptavidin R-PE (1:500; catalog number 922721; Qiagen). Samples were washed and resuspended in 100 μl PBS. Finally, flow cytometry was performed with a BD LSR II flow cytometer (BD Bioscience), and FlowJo software (Tree Star, San Carlos, CA, USA) was used for data analysis.

Histology. Mice was euthanized, and the liver was perfused with PBS and extracted. The tissues were subsequently fixed overnight in 4% paraformaldehyde at 4°C with gentle agitation and then dehydrated overnight in cryoprotection solution (30% sucrose solution, PBS) at 4°C with gentle agitation before they were embedded in OCT specimen matrix compound for frozen sectioning. Liver cryosections 6 μm thick were cut on a microtome and treated with a solution containing 5% bovine serum albumin and 0.5% Triton X-100 for 1 h for blocking and permeabilization. Liver sections were stained with anti-claudin-1 (1:200; Invitrogen), anti-occludin (1:200; Invitrogen), or anti-ZO-1 (1:200; Thermo Fisher Scientific) primary antibodies for 16 h. After the liver sections were washed with PBS, they were stained with secondary Alexa Fluor 647-conjugated goat anti-mouse or anti-rabbit immunoglobulin antibodies (1:500; Thermo Fisher Scientific) for 2 h. Nuclei were stained with Hoechst dye. Liver sections were then washed three times for 5 min each time with PBS. The slides were mounted by the use of mounting solution, and images were acquired by a Nikon A1 spectral confocal microscope.

Bioluminescence imaging. Rosa26-Fluc, entry factor transgenic Rosa26-Fluc (EFT Rosa26-Fluc), and mCD81/hEL2[h/h] mOCLN/hEL2[h/h] Rosa26-Fluc mice were injected intravenously with the doses of HCV-Cre indicated below. Rosa26-Fluc mice were injected with 10^{11} PFU of adenovirus 24 h prior to intravenous injection of 2×10^7 $TCID_{50}$ HCV-Cre. At 72 h postinfection, mice were anesthetized using ketamine-xylazine and injected intraperitoneally with 1.5 mg luciferin (Caliper Life Sciences). For the *ex vivo* measurement of luciferase activity across different tissues, the organs indicated above were extracted from mCD81/hEL2[h/h] mOCLN/hEL2[h/h] Rosa26-Fluc at 72 h postinfection and placed in PBS containing luciferin (0.15 mg/ml), and luminescent activity was measured. Bioluminescence was measured using an Ivis Lumina II platform (Caliper Life Sciences).

ACKNOWLEDGMENTS

We thank Jenna Gaska for edits and critical discussion of the manuscript.

This study is supported by grants from the National Institutes of Health (R01 AI079031, R01 AI107301, and R21AI117213 to A.P.), a research scholar award from the American Cancer Society (RSG-15-048-01-MPC to A.P.), and a Burroughs Wellcome Fund Award for Investigators in Pathogenesis (to A.P.). Q.D. is a recipient of a postdoctoral fellowship from the New Jersey Commission on Cancer Research,

and M.V.S. is a recipient of a postdoctoral fellowship from the German Research Foundation (Deutsche Forschungsgemeinschaft). L.S. is a fellow of the German National Merit Foundation and was supported by a stipend from the Organization of Supporters of the Hannover Medical School (Gesellschaft der Freunde der Medizinischen Hochschule Hannover e.V.).

REFERENCES

1. Lindenbach BD, Rice CM. 2001. *Flaviviridae*: the viruses and their replication, p 991–1041. *In* Knipe DM, Howley PM, Griffin D, Lamb R, Martin M, Straus S (ed), Fields virology, 4th ed, vol 1. Lippincott Williams & Wilkins, Philadelphia, PA.
2. Westbrook RH, Dusheiko G. 2014. Natural history of hepatitis C. J Hepatol 61:S58–S68. https://doi.org/10.1016/j.jhep.2014.07.012.
3. Wang LS, D'Souza LS, Jacobson IM. 2016. Hepatitis C—a clinical review. J Med Virol 88:1844–1855. https://doi.org/10.1002/jmv.24554.
4. von Schaewen M, Ploss A. 2014. Murine models of hepatitis C: what can we look forward to? Antiviral Res 104:15–22. https://doi.org/10.1016/j.antiviral.2014.01.007.
5. Ding Q, von Schaewen M, Ploss A. 2014. The impact of hepatitis C virus entry on viral tropism. Cell Host Microbe 16:562–568. https://doi.org/10.1016/j.chom.2014.10.009.
6. Barth H, Schafer C, Adah MI, Zhang F, Linhardt RJ, Toyoda H, Kinoshita-Toyoda A, Toida T, Van Kuppevelt TH, Depla E, Von Weizsacker F, Blum HE, Baumert TF. 2003. Cellular binding of hepatitis C virus envelope glycoprotein E2 requires cell surface heparan sulfate. J Biol Chem 278:41003–41012. https://doi.org/10.1074/jbc.M302267200.
7. Agnello V, Abel G, Elfahal M, Knight GB, Zhang QX. 1999. Hepatitis C virus and other flaviviridae viruses enter cells via low density lipoprotein receptor. Proc Natl Acad Sci U S A 96:12766–12771. https://doi.org/10.1073/pnas.96.22.12766.
8. Pileri P, Uematsu Y, Campagnoli S, Galli G, Falugi F, Petracca R, Weiner AJ, Houghton M, Rosa D, Grandi G, Abrignani S. 1998. Binding of hepatitis C virus to CD81. Science 282:938–941. https://doi.org/10.1126/science.282.5390.938.
9. Scarselli E, Ansuini H, Cerino R, Roccasecca RM, Acali S, Filocamo G, Traboni C, Nicosia A, Cortese R, Vitelli A. 2002. The human scavenger receptor class B type I is a novel candidate receptor for the hepatitis C virus. EMBO J 21:5017–5025. https://doi.org/10.1093/emboj/cdf529.
10. Evans MJ, von Hahn T, Tscherne DM, Syder AJ, Panis M, Wolk B, Hatzioannou T, McKeating JA, Bieniasz PD, Rice CM. 2007. Claudin-1 is a hepatitis C virus co-receptor required for a late step in entry. Nature 446:801–805. https://doi.org/10.1038/nature05654.
11. Liu S, Yang W, Shen L, Turner JR, Coyne CB, Wang T. 2009. Tight junction proteins claudin-1 and occludin control hepatitis C virus entry and are downregulated during infection to prevent superinfection. J Virol 83:2011–2014. https://doi.org/10.1128/JVI.01888-08.
12. Ploss A, Evans MJ, Gaysinskaya VA, Panis M, You H, de Jong YP, Rice CM. 2009. Human occludin is a hepatitis C virus entry factor required for infection of mouse cells. Nature 457:882–886. https://doi.org/10.1038/nature07684.
13. Lupberger J, Zeisel MB, Xiao F, Thumann C, Fofana I, Zona L, Davis C, Mee CJ, Turek M, Gorke S, Royer C, Fischer B, Zahid MN, Lavillette D, Fresquet J, Cosset FL, Rothenberg SM, Pietschmann T, Patel AH, Pessaux P, Doffoel M, Raffelsberger W, Poch O, McKeating JA, Brino L, Baumert TF. 2011. EGFR and EphA2 are host factors for hepatitis C virus entry and possible targets for antiviral therapy. Nat Med 17:589–595. https://doi.org/10.1038/nm.2341.
14. Sainz B, Jr, Barretto N, Martin DN, Hiraga N, Imamura M, Hussain S, Marsh KA, Yu X, Chayama K, Alrefai WA, Uprichard SL. 2012. Identification of the Niemann-Pick C1-like 1 cholesterol absorption receptor as a new hepatitis C virus entry factor. Nat Med 18:281–285. https://doi.org/10.1038/nm.2581.
15. Martin DN, Uprichard SL. 2013. Identification of transferrin receptor 1 as a hepatitis C virus entry factor. Proc Natl Acad Sci U S A 110:10777–10782. https://doi.org/10.1073/pnas.1301764110.
16. Wu X, Lee EM, Hammack C, Robotham JM, Basu M, Lang J, Brinton MA, Tang H. 2014. Cell death-inducing DFFA-like effector b is required for hepatitis C virus entry into hepatocytes. J Virol 88:8433–8444. https://doi.org/10.1128/JVI.00081-14.
17. Li Q, Sodroski C, Lowey B, Schweitzer CJ, Cha H, Zhang F, Liang TJ. 2016. Hepatitis C virus depends on E-cadherin as an entry factor and regulates its expression in epithelial-to-mesenchymal transition. Proc Natl Acad Sci U S A 113:7620–7625. https://doi.org/10.1073/pnas.1602701113.
18. Higginbottom A, Quinn ER, Kuo CC, Flint M, Wilson LH, Bianchi E, Nicosia A, Monk PN, McKeating JA, Levy S. 2000. Identification of amino acid residues in CD81 critical for interaction with hepatitis C virus envelope glycoprotein E2. J Virol 74:3642–3649. https://doi.org/10.1128/JVI.74.8.3642-3649.2000.
19. Michta ML, Hopcraft SE, Narbus CM, Kratovac Z, Israelow B, Sourisseau M, Evans MJ. 2010. Species-specific regions of occludin required by hepatitis C virus for cell entry. J Virol 84:11696–11708. https://doi.org/10.1128/JVI.01555-10.
20. Vogt A, Scull MA, Friling T, Horwitz JA, Donovan BM, Dorner M, Gerold G, Labitt RN, Rice CM, Ploss A. 2013. Recapitulation of the hepatitis C virus life-cycle in engineered murine cell lines. Virology 444:1–11. https://doi.org/10.1016/j.virol.2013.05.036.
21. Dorner M, Horwitz JA, Robbins JB, Barry WT, Feng Q, Mu K, Jones CT, Schoggins JW, Catanese MT, Burton DR, Law M, Rice CM, Ploss A. 2011. A genetically humanized mouse model for hepatitis C virus infection. Nature 474:208–211. https://doi.org/10.1038/nature10168.
22. Dorner M, Horwitz JA, Donovan BM, Labitt RN, Budell WC, Friling T, Vogt A, Catanese MT, Satoh T, Kawai T, Akira S, Law M, Rice CM, Ploss A. 2013. Completion of the entire hepatitis C virus life cycle in genetically humanized mice. Nature 501:237–241. https://doi.org/10.1038/nature12427.
23. Giang E, Dorner M, Prentoe JC, Dreux M, Evans MJ, Bukh J, Rice CM, Ploss A, Burton DR, Law M. 2012. Human broadly neutralizing antibodies to the envelope glycoprotein complex of hepatitis C virus. Proc Natl Acad Sci U S A 109:6205–6210. https://doi.org/10.1073/pnas.1114927109.
24. Anggakusuma, Colpitts CC, Schang LM, Rachmawati H, Frentzen A, Pfaender S, Behrendt P, Brown RJ, Bankwitz D, Steinmann J, Ott M, Meuleman P, Rice CM, Ploss A, Pietschmann T, Steinmann E. 2014. Turmeric curcumin inhibits entry of all hepatitis C virus genotypes into human liver cells. Gut 63:1137–1149. https://doi.org/10.1136/gutjnl-2012-304299.
25. de Jong YP, Dorner M, Mommersteeg MC, Xiao JW, Balazs AB, Robbins JB, Winer BY, Gerges S, Vega K, Labitt RN, Donovan BM, Giang E, Krishnan A, Chiriboga L, Charlton MR, Burton DR, Baltimore D, Law M, Rice CM, Ploss A. 2014. Broadly neutralizing antibodies abrogate established hepatitis C virus infection. Sci Transl Med 6:254ra129. https://doi.org/10.1126/scitranslmed.3009512.
26. Silvie O, Rubinstein E, Franetich JF, Prenant M, Belnoue E, Renia L, Hannoun L, Eling W, Levy S, Boucheix C, Mazier D. 2003. Hepatocyte CD81 is required for Plasmodium falciparum and Plasmodium yoelii sporozoite infectivity. Nat Med 9:93–96.
27. Maecker HT, Levy S. 1997. Normal lymphocyte development but delayed humoral immune response in CD81-null mice. J Exp Med 185:1505–1510. https://doi.org/10.1084/jem.185.8.1505.
28. Tsitsikov EN, Gutierrez-Ramos JC, Geha RS. 1997. Impaired CD19 expression and signaling, enhanced antibody response to type II T independent antigen and reduction of B-1 cells in CD81-deficient mice. Proc Natl Acad Sci U S A 94:10844–10849. https://doi.org/10.1073/pnas.94.20.10844.
29. Miyazaki T, Muller U, Campbell KS. 1997. Normal development but differentially altered proliferative responses of lymphocytes in mice lacking CD81. EMBO J 16:4217–4225. https://doi.org/10.1093/emboj/16.14.4217.
30. Van Itallie CM, Anderson JM. 2014. Architecture of tight junctions and principles of molecular composition. Semin Cell Dev Biol 36:157–165. https://doi.org/10.1016/j.semcdb.2014.08.011.
31. Saitou M, Furuse M, Sasaki H, Schulzke JD, Fromm M, Takano H, Noda T, Tsukita S. 2000. Complex phenotype of mice lacking occludin, a com-

ponent of tight junction strands. Mol Biol Cell 11:4131–4142. https://doi.org/10.1091/mbc.11.12.4131.
32. Dorner M, Rice CM, Ploss A. 2013. Study of hepatitis C virus entry in genetically humanized mice. Methods 59:249–257. https://doi.org/10.1016/j.ymeth.2012.05.010.
33. von Schaewen M, Ding Q, Ploss A. 2014. Visualizing hepatitis C virus infection in humanized mice. J Immunol Methods 410:50–59. https://doi.org/10.1016/j.jim.2014.03.006.
34. Safran M, Kim WY, Kung AL, Horner JW, DePinho RA, Kaelin WG, Jr. 2003. Mouse reporter strain for noninvasive bioluminescent imaging of cells that have undergone Cre-mediated recombination. Mol Imaging 2:297–302. https://doi.org/10.1162/153535003322750637.
35. Xie ZC, Riezu-Boj JI, Lasarte JJ, Guillen J, Su JH, Civeira MP, Prieto J. 1998. Transmission of hepatitis C virus infection to tree shrews. Virology 244:513–520. https://doi.org/10.1006/viro.1998.9127.
36. Xu X, Chen H, Cao X, Ben K. 2007. Efficient infection of tree shrew (Tupaia belangeri) with hepatitis C virus grown in cell culture or from patient plasma. J Gen Virol 88:2504–2512. https://doi.org/10.1099/vir.0.82878-0.
37. Amako Y, Tsukiyama-Kohara K, Katsume A, Hirata Y, Sekiguchi S, Tobita Y, Hayashi Y, Hishima T, Funata N, Yonekawa H, Kohara M. 2010. Pathogenesis of hepatitis C virus infection in Tupaia belangeri. J Virol 84:303–311. https://doi.org/10.1128/JVI.01448-09.
38. Pfaender S, Brown RJ, Pietschmann T, Steinmann E. 2014. Natural reservoirs for homologs of hepatitis C virus. Emerg Microbes Infect 3:e21. https://doi.org/10.1038/emi.2014.19.
39. Mercer DF, Schiller DE, Elliott JF, Douglas DN, Hao C, Rinfret A, Addison WR, Fischer KP, Churchill TA, Lakey JR, Tyrrell DL, Kneteman NM. 2001. Hepatitis C virus replication in mice with chimeric human livers. Nat Med 7:927–933. https://doi.org/10.1038/90968.
40. Meuleman P, Libbrecht L, De Vos R, de Hemptinne B, Gevaert K, Vandekerckhove J, Roskams T, Leroux-Roels G. 2005. Morphological and biochemical characterization of a human liver in a uPA-SCID mouse chimera. Hepatology 41:847–856. https://doi.org/10.1002/hep.20657.
41. Bissig KD, Wieland SF, Tran P, Isogawa M, Le TT, Chisari FV, Verma IM. 2010. Human liver chimeric mice provide a model for hepatitis B and C virus infection and treatment. J Clin Invest 120:924–930. https://doi.org/10.1172/JCI40094.
42. Forton DM, Taylor-Robinson SD, Thomas HC. 2003. Cerebral dysfunction in chronic hepatitis C infection. J Viral Hepat 10:81–86. https://doi.org/10.1046/j.1365-2893.2003.00416.x.
43. Fishman SL, Murray JM, Eng FJ, Walewski JL, Morgello S, Branch AD. 2008. Molecular and bioinformatic evidence of hepatitis C virus evolution in brain. J Infect Dis 197:597–607. https://doi.org/10.1086/526519.
44. Burgel B, Friesland M, Koch A, Manns MP, Wedemeyer H, Weissenborn K, Schulz-Schaeffer WJ, Pietschmann T, Steinmann E, Ciesek S. 2011. Hepatitis C virus enters human peripheral neuroblastoma cells—evidence for extra-hepatic cells sustaining hepatitis C virus penetration. J Viral Hepat 18:562–570. https://doi.org/10.1111/j.1365-2893.2010.01339.x.
45. Fletcher NF, Yang JP, Farquhar MJ, Hu K, Davis C, He Q, Dowd K, Ray SC, Krieger SE, Neyts J, Baumert TF, Balfe P, McKeating JA, Wong-Staal F. 2010. Hepatitis C virus infection of neuroepithelioma cell lines. Gastroenterology 139:1365–1374. https://doi.org/10.1053/j.gastro.2010.06.008.
46. Marukian S, Jones CT, Andrus L, Evans MJ, Ritola KD, Charles ED, Rice CM, Dustin LB. 2008. Cell culture-produced hepatitis C virus does not infect peripheral blood mononuclear cells. Hepatology 48:1843–1850. https://doi.org/10.1002/hep.22550.
47. Deforges S, Evlashev A, Perret M, Sodoyer M, Pouzol S, Scoazec JY, Bonnaud B, Diaz O, Paranhos-Baccala G, Lotteau V, Andre P. 2004. Expression of hepatitis C virus proteins in epithelial intestinal cells in vivo. J Gen Virol 85:2515–2523. https://doi.org/10.1099/vir.0.80071-0.
48. Mee CJ, Grove J, Harris HJ, Hu K, Balfe P, McKeating JA. 2008. Effect of cell polarization on hepatitis C virus entry. J Virol 82:461–470. https://doi.org/10.1128/JVI.01894-07.
49. Kohaar I, Ploss A, Korol E, Mu K, Schoggins JW, O'Brien TR, Rice CM, Prokunina-Olsson L. 2010. Splicing diversity of the human OCLN gene and its biological significance for hepatitis C virus entry. J Virol 84:6987–6994. https://doi.org/10.1128/JVI.00196-10.
50. Lindenbach BD, Evans MJ, Syder AJ, Wolk B, Tellinghuisen TL, Liu CC, Maruyama T, Hynes RO, Burton DR, McKeating JA, Rice CM. 2005. Complete replication of hepatitis C virus in cell culture. Science 309:623–626. https://doi.org/10.1126/science.1114016.
51. Schoggins JW, Gall JG, Falck-Pedersen E. 2003. Subgroup B and F fiber chimeras eliminate normal adenovirus type 5 vector transduction in vitro and in vivo. J Virol 77:1039–1048. https://doi.org/10.1128/JVI.77.2.1039-1048.2003.